Mechanism and Machine Theory 185 (2023) 105334

Contents lists available at ScienceDirect

Mechanism and Machine Theory

journal homepage: www.elsevier.com/locate/mechmt

Research paper

An analytical solution of the rope-sheave contact in static conditions based on a bristle model

José L. Escalona

Department of Mechanical and Manufacturing Engineering, University of Seville, Spain

ARTICLE INFO

Keywords:
Contact mechanics
Reeving systems
Rope-sheave contact

ABSTRACT

This paper presents an analytical solution for the rope-sheave contact problem in static conditions, also applicable to belt-pulley problems and similar mechanisms. The rope is assumed under constant and unequal loads at the two ends, as in an elevator when the brake is acting on the drive sheave and the weights of the cabin and counterweights are different. The rope is assumed to behave as a rod without bending stiffness. Assuming a bristle model for the rope-sheave contact and Coulomb friction, the balance of forces in a differential slice of the rope is used to obtain a closed-form solution for the axial force field and the normal and tangential contact force fields. This analytical solution is found first in the case of a bristle model with tangential flexibility but axially rigid. Then, the model is extended to axially flexible bristles, that allows the rope to sheave relative penetration. The solution is valid until one cross-section of the rope achieves the saturated tangential friction force. The value of the axial load when this condition is met is identified. If the high-load further increases, the rope in contact with the sheave is separated in two areas, the area next to the low-load remains fully stuck to the sheave while the area next to the high-load shows exactly the saturated friction force. This paper calculates the angle of separation between the two areas and the axial force field and normal and tangential contact force fields, being all these functions piece-wisely defined. Finally, the paper presents numerical results for a particular example of all the analytical solutions.

1. Introduction

When entering the cabin of an elevator, before it starts moving, a brake is acting on the drive sheave. After pressing the button of the floor where we want to go, the brake opens while the electric drive applies a torque that initially balances the weight difference between the cabin and the counterweight, thus avoiding the free fall or free rise of the cabin that would happen depending on the relative weight of the cabin and the counterweight. Afterwards, the electric drive modifies the torque to get the required acceleration to start the motion. Motion, force and power are transmitted in this process through the normal and tangential contact stresses at the rope-sheave interface. It is apparent the need to understand the rope-sheave contact problem. Surprisingly, a simple analytical solution of the rope-sheave contact problem is well known under dynamic conditions, when the drive sheave is rotating, but there are no analytical solutions, to the best knowledge of the author, under static conditions. The dynamic analytical solution of the rope-sheave contact problem is the same as the *Euler-Eytelwin formula* also known as *capstan formula* or belt friction problem [1,2]. This solution is used in the European standard EN 81-1 [3] that deals with safety in electric elevators. However, this solution may not be very accurate for the rope-sheave contact. That is probably why the standard proposes to consider a very low coefficient of friction, smaller than 0.1, as a safety factor to compensate for the uncertainty in the applied theory.

E-mail address: escalona@us.es.

https://doi.org/10.1016/j.mechmachtheory.2023.105334
Received 12 December 2022; Received in revised form 3 March 2023; Accepted 15 March 2023
Available online 29 March 2023

In the instant when the user enters the cabin, although the brake is acting, this device just guarantees that the drive sheave does not rotate. However, by no means the brake grasps the wire ropes to avoid the rope to sheave relative slipping. This is, we trust that dry friction is able to keep the cabin still but, if we ask the elevator designer how much mass could enter the cabin before rope to sheave slip starts, probably the designer would say that that depends on the coefficient of friction. But the coefficient of friction is not known accurately. Therefore, the amount of load that rope-sheave friction can withstand is not clear. Even if the coefficient of friction is accurately known, there is no theory that tells you under which load rope slipping will start before the gross slipping happens. The Euler-Eytelwin formula is not applicable under static conditions. This situation may look scary, but it is totally real. For the peace of the reader we will say that modern elevators have safety brakes that, if the cabin starts falling too fast, a mechanism called *governor* detects it and activates a device that clamps the cabin to the rail guides.

Euler-Eitelwing formula was applied to the analysis of belt-pulley transmission mechanisms by Reynolds and Grashof. In 1875 Reynolds [4] added the effect of speed loss in the belt due to the micro-slip and in 1883 Grashof [5] included the effect of the centrifugal force. The theory of force transmission in belt drives was called afterwards *Reynolds-Grashof theory* or *belt creep theory*. New developments of the belt-pulley contact theory were published by Firbank in 1970 [6] motivated by the use in the industry of belts with a soft pliable envelope to grip the pulley and strong tension members to transmit the power. In this type of pulley, the belt deformation was mainly due to shear deformation of the envelope instead of axial deformation of the tension members. Firbank theory assumes the belt to be inextensible. His theory showed the existence of slip and adherence arcs, as in Reynolds-Grashof theory, but the slip arc was shown to be also capable of transmitting power. Recently, Frendo and Bucchi have developed an analytical and numerical study of the contact forces in belt transmissions, based on the brush model, that is able to catch the stick–slip contact behaviour that has been experimentally observed. Their model was first developed for axially rigid belts [7] and later they included the axial flexibility [8]. This model has been validated with a finite element model [9]. Chowdhury and Yedavalli [10] developed an analytical model of a belt transmission system for vibration analysis. The shafts of the pulleys are considered as continuous beams with torsional flexibility and the belt is treated as a combination of linear and torsional springs. This model is used to develop a detail vibration analysis of the transmission system using Campbell diagrams and modal energy plots.

In the rope-sheave contact analysis, few advances were done in the scientific literature since Euler-Eitelwing seminal work. In 1970 Heller published [11] a rope-sheave contact theory considering the effect of the shear forces in the rope and accounting for the rope diameter to sheave diameter ratio. Results were only applicable to the slip arc. Heller studied the effect of the rope weight and the angular velocity of the sheave in the contact force distributions. Feyrer [12] studied the tape-sheave contact and the rope-sheave contact in static conditions. In the case of the tape-sheave contact, the normal contact force distribution is approximated as a constant value, equal to the applied axial force on the tape divided by the radius of the sheave, plus two concentrated normal forces applied at the ends of the contact region. These concentrated forces are calculated analytically as function of the applied axial force and the bending stiffness of the tape. In the case of the rope-sheave contact, Feyrer shows that the concentrated forces at the ends of the contact region turn into finite regions in the contact bow where the normal pressure increases its value with a pressure peak that is about 50% higher than in the remaining of the bow. Feyrer does not study the tangential contact stress distribution and its influence in the normal contact pressures distribution of the rope-sheave contact. Konyukhov [13] published a paper about the contact of ropes on orthotropic rough surfaces. For a rope in contact with a general surfaces, he derives the variational equation of equilibrium including the frictional contact constraints via Karush–Kuhn–Tucker conditions. Using these general equations, various cases possessing analytical solutions are presented, like the Euler-Eytelwin solution.

Regarding experimental studies, using a belt-testing machine, Firbank [6] showed that the contact theory based on shear deformation of the rubber reinforced belts was much more accurate than the Reynolds-Grashof theory. Experiments showed that the creep to tension difference plot based on the shear deformation theory agrees reasonably well with experimental results. Häberle [14] measured the effect in the contact pressure of the bending stiffness of the ropes, that is known to create relatively high peaks at the entrance and running of points of the rope in the sheave. Häberle made measurements of the ratio of the maximum and the global line pressures as a function of the diameter ratio of the sheave and the rope. Nabijou and Hobbs [15] studied the rope-sheave effective coefficient of friction in static and dynamic case. To do that, in their test rig, they were able to measure the load transmitted to the two rope spans. They did experiments to analyse many different effects including the profile of the sheave groove, the pulley diameter, the rope diameter to sheave diameter ratio, the rope and pulley use and the effect of rope internal construction. Usabiaga et al. [16] built an experimental setup in which the were able to insert a 3D piezoelectric load cell in a thin sector of a drive sheave. With this cell, they experimentally measured the rope-sheave normal and tangential contact pressure fields. They did it with conventional ropes and jacketed ropes. They measured the pressures peaks at the entrance and running of points at the sheave. They concluded that the pressure fields match relatively well Heller theory [11] for conventional ropes, but the jacketed rope showed an different normal and tangential contact force field that they attributed to the effect of the shear stress in the jacket. Della Pietra and Timpone [17] measured the tension of belts using strain gauges installed in the outer surface of a flat belt in a transmission. They compared the results with Reynolds-Grashof theory and Firbank theory. They confirm the presence of the adhesion and slipping arcs. Adhesion arc appeared at the entrance of the driving and driving pulleys, and the tension of the belt in these arcs appeared to be constant, what is consistent with Reynolds-Grashof theory. Experiments also showed the presence of shear strain and different sliding angles in the driving and driven pulleys, as Firbank theory predicts. Recently, Lee et al. [18] have developed a model to predict the position of a load suspended on a viscoelastic winch-driven rope. The rope-sheave contact was modelled using Firbank theory. The model was experimentally validated with a laboratory test bench.

In computational mechanics, belt-pulley problems [19–24] or rope-sheave problems [25–28] are solved to analyse the dynamics of power transmission systems or reeving systems. Belts and ropes use to be modelled using finite elements, being the *Absolute Nodal Coordinate Formulation*, that was developed for the analysis of large deformation of flexible multibody systems [29], very well suited

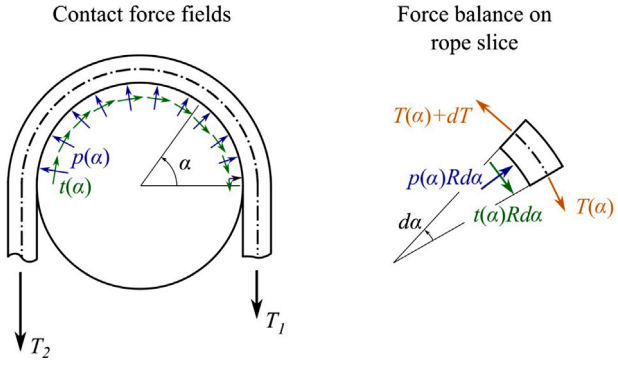

Fig. 1. Rope-sheave contact.

for these applications [20,25,26]. These problems can also been solved using an *Arbitrary Lagrangian–Eulerian Formulation* [30–32] that offers important advantages for the simulation of general reeving systems with improved computational efficiency and accuracy. Regarding the friction models, belt-pulley problems in power transmission mechanism and rope-sheave problems in reeving systems have to be treated differently. In belt-pulley problems, steady states or transients about a steady velocity use to be of interest. To that end, *velocity-based friction models* (or *creep models* or *micro-slip models*) work very well. The problem is that when using velocity-based models friction is zero when the relative slip velocity of the solids in contact is zero. Thus, these models cannot describe static equilibrium positions in hoisting machines, like the case of the elevator that was mentioned before. In reeving systems, particularly in problems like elevators and cranes, the assumed friction model in the rope-sheave interface has to be able to generate friction forces when the slip velocity is zero. To this end, *bristle models* [33], also called *brush models*, can be used. Bristle models can be used to calculate friction forces under stick and slip conditions. However, when used for dynamic simulations, these models create problems because the number of generalized coordinates vary depending on whether the bristles are stuck or slip. This problem can be solved using the *LuGre friction model* [34] that regularizes the stick–slip friction problems such that there is no sudden transition, but in an imaginary state in with the contact points stick and slip at the same time.

This paper presents a very simple analytical solution of the rope-sheave contact problem for static analysis. It is based on the solution of the differential balance equations of a continuous planar elastic rod on a circular surface. The bristle model is used to account for dry friction. The solution depends on a few parameters: the loads at the two ends of the rope, the coefficient of friction, the radius of the sheave, the axial stiffness of the rod and the normal and tangential stiffness of the bristles. Compared with the belt-pulley and rope-sheave contact theories that have been described, the approach presented in this paper provides an analytical solution under static conditions, when all these theories are not applicable, because dynamic friction is not possible and creep or slipping does not occur. The static condition is very important in hoisting machines, as described in the first two paragraph of this introduction. The model used in this work considers the rope as an elastic rope without bending stiffness. The shear deformation of the rope is accounted for using a bristle model, that is suitable to describe static and dynamic friction. This approach for modelling shear deformation is not new, as it is equivalent to the classical model developed by Firbank [6] and the brush model recently used by Frendo and Bucchi [8]. However, these investigations were applied to belt transmissions and did not consider the static case.

This paper is organized as follows. Section 2 presents the differential balance equations of a rod in contact with a circular surface and the Euler-Eytelwin solution applied to a simple elevator problem. Section 3 presents the analytical solution based on the bristle model. Two cases are considered: the case of bristles that are only transversely flexible and the case of bristles that are axially flexible too. This section also demonstrate the validity of the presented solutions through the application the *Principle of Work and Energy*. Section 4 establishes the limits of the proposed solution at the on-set of rope to sheave slipping and the contact conditions when the rope partially slips on the sheave. Section 5 presents a numerical example of all the solutions obtained in the paper. Finally, summary and conclusions are given in Section 6.

2. Euler-eytelwin solution in steady dynamic problems

The system under consideration is shown in Fig. 1. In this paper it will be assumed that the contact angle between the rope and the sheave is 180°, however, the results can be easily extended to any angle. The rope is modelled as a linear elastic rod with axial stiffness EA and mass-less. The axial force along the rope T is known at the two ends of the rope, being their values T_1 and T_2, with $T_1 \leq T_2$. The variation of the axial force varies along the contact angle is considered a function of the contact angle α, this is, $T = T(\alpha)$. In the rope-sheave interface there exit a normal contact pressure distribution $p(\alpha)$ and a tangential contact force distribution $t(\alpha)$ (units of both distributions are N/m). In the following, the axial force $T(\alpha)$ and contact forces $p(\alpha)$ and $t(\alpha)$ will be calculated as a function of the system parameters.

Fig. 1 on the right shows an infinitesimal slice of the rope in contact with the sheave and the forces acting on it. For convenience, the tangential contact forces $t(\alpha)$ acting on the rope are defined positive when acting on the contrary direction of α. Force balance

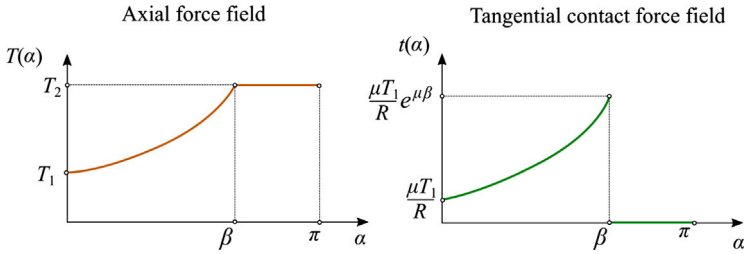

Fig. 2. Solution under dynamic conditions. Axial force and tangential contact force distributions at rope-sheave interface.

in the radial and tangential directions yields:

$$\left.\begin{array}{l} p(\alpha)\, R d\alpha = T(\alpha)\, d\alpha \\ t(\alpha)\, R d\alpha = dT \end{array}\right\} \Rightarrow \left\{\begin{array}{l} p(\alpha) = \frac{1}{R} T(\alpha) \\ t(\alpha) = \frac{1}{R}\frac{dT(\alpha)}{d\alpha} \end{array}\right. \tag{1}$$

Therefore, the normal pressure is proportional to the axial force and the tangential contact force is proportional to the space derivative of the axial force.

In the case of dynamic contact, this is, when the sheave rotates with a finite angular velocity, these equilibrium equations together with Coulomb friction law can be used to obtain the normal and tangential contact force distributions and the axial force distribution as a function of the axial forces at the ends T_1 and T_2 , being ends 1 and 2 the cross-sections of the rope at the ends of the segment winded in the sheave. Without loss of generality, assume that tensile force T_2 is larger than T_1, and the sheave angle α is measures starting at end 1. In such a case, there is a finite arc at the sheave $\alpha \in \left[\begin{array}{cc} 0 & \beta \end{array}\right]$ next to end 1 where the rope slips over the sheave. The axial force distribution in this sliding arc is obtained as follows:

$$\begin{array}{l} |t(\alpha)| = \mu p(\alpha) \Rightarrow \frac{1}{R}\frac{dT(\alpha)}{d\alpha} = \frac{\mu}{R} T(\alpha) \Rightarrow \frac{dT(\alpha)}{T(\alpha)} = \mu d\alpha \Rightarrow \\ \qquad T(\alpha) = T_1 e^{\mu\alpha} \end{array} \tag{2}$$

where the force balance given in Eq. (1) has been used and the derivative of T with respect to α has been assumed to be positive. This is the Euler-Eytelwin formula that is applicable in the so-called *slip arc*. This arc ends at $\alpha = \beta$. The value of β that can be obtained using the boundary condition at the other end of the rope, as follows:

$$T_1 e^{\mu\beta} = T_2 \Rightarrow \beta = \frac{1}{\mu} \log \frac{T_2}{T_1} \tag{3}$$

If this formula gives an angle β is larger than 180°, the result is clearly physically impossible. This result indicate a gross slipping (opposite to the micro-slip or creep that happens in the slip arc) of the rope over the sheave. This result is used in the elevator industry [3] to limit the axial force difference at the two ends of the traction ropes. Using this result, the maximum axial force at $\alpha = \pi$ when gross slipping starts is be obtained as:

$$\frac{1}{\mu} \log \frac{T_2^{gross}}{T_1} = \pi \quad \Rightarrow \quad T_2^{gross} = T_1 e^{\mu\pi} \tag{4}$$

This equation is not applicable in static conditions because the dynamic friction force considered in Eq. (2) is not possible.

In the rest of the rope-sheave contact arc $\alpha \in \left[\begin{array}{cc} \beta & \pi \end{array}\right]$ the rope is stuck at the sheave. In this contact arc the axial force along the rope remains constant and equal to T_2 and the tangential contact force distribution $t(\alpha)$ vanishes. The distribution of axial force and tangential contact force yield (Fig. 2):

$$T(\alpha) = \left\{\begin{array}{c} T_1 e^{\mu\alpha}, \alpha \in \left[\begin{array}{cc} 0 & \beta \end{array}\right] \\ T_2, \alpha \in \left[\begin{array}{cc} \beta & \pi \end{array}\right] \end{array}\right. , t(\alpha) = \left\{\begin{array}{c} \frac{\mu T_1}{R} e^{\mu\alpha}, \alpha \in \left[\begin{array}{cc} 0 & \beta \end{array}\right] \\ 0, \alpha \in \left[\begin{array}{cc} \beta & \pi \end{array}\right] \end{array}\right. \tag{5}$$

From these results very interesting conclusions can be taken when sheave is rotating and the system is moving in steady conditions:

1. Unless the axial forces at both ends of the rope are the same, there is always a slip arc in the rope-sheave interface.
2. All the forces that drive the system (raise the cabin and lower the counterweight or vice-versa) are transmitted in that slip arc. In the stick arc drive forces are not transmitted.

To account for the acceleration and deceleration periods, in the elevator industry these equations are used considering as end forces T_1 and T_2 the sum of the weights of the cabin and counterweight plus the inertia forces that result when considering the no-slip condition. This way, the maximum allowed acceleration and deceleration of the elevator system can be estimated.

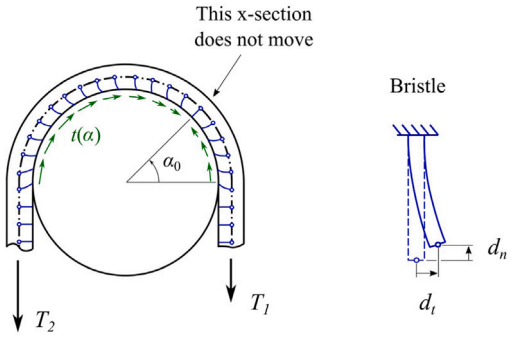

Fig. 3. Rope-sheave contact modelled with bristles.

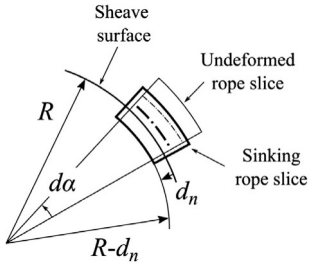

Fig. 4. Rope slice sinking in the sheave.

3. Analytical solution of the rope-sheave contact in static conditions

The results presented in the previous section have been known for many years and nowadays they are widely used machine design. However, the results are not applicable under static conditions.

Under static conditions, it can be considered that the rope is stuck to the sheave. However, the tangential contact force cannot be zero as it is in Euler-Eytelwin solution in the stuck area because the tangential contact forces have to balance the load difference at the two ends of the rope. Coulomb friction theory does not provide any formula to calculate the tangential contact force in the case of stick contact. In rigid body mechanics, the static tangential contact force must be treated as a reaction force with a maximum possible value, the saturated tangential force that equals the coefficient of friction times the normal contact force. In order to solve the tangential contact force field in static conditions, a formula that relates the tangential contact force to the rope elasticity is needed. In this work, this formula is provided by the bristle model [33].

Fig. 3 is a graphical representation of the bristle model applied to the rope-sheave contact problem. The rope is assumed to have a set of bristles that are cantilevered to the centreline and their free ends touch the surface of the sheave. The bristles deform in the normal and tangential directions, as shown in the right of Fig. 3. The bristles are assumed linear elastic, such that the normal and tangential forces generated by the bristle are proportional to the normal deformation d_n and tangential deformation d_t, respectively. Assume now that the bristles are not discrete but there is a continuous distribution of bristles along the rope. In this case, the normal and tangential contact force distributions can be obtained as:

$$\begin{aligned} t(\alpha) &= k_t d_t(\alpha), \\ p(\alpha) &= k_n d_n(\alpha) \end{aligned} \tag{6}$$

where k_t and k_n are the tangential and normal stiffness of the bristles.

Fig. 4 shows the model of an infinitesimal slice of the rope in contact with the sheave. The normal stiffness of the bristles prevents the slice to sink into the surface of the sheave. If the bristles are assumed to be rigid in the axial direction ($k_n \to \infty$), as done in the following subsection, the rope does not sink into the sheave ($d_n = 0$).

3.1. Analytical solution with laterally elastic bristles

Assume that the bristles are elastic in the lateral direction but rigid in the axial direction. Because the free ends of the bristles are stuck to the sheave, the lateral deformation equals the longitudinal displacement of the attachment point at the rope centreline, this is, $d_t(\alpha) = u(\alpha)$, where u is the displacement of the centreline due to the rope elasticity. This formula can be used to relate the tangential contact force to the axial force, as follows:

$$t(\alpha) = k_t u(\alpha) \;\Rightarrow\; \frac{dt}{ds} = k_t \frac{du}{ds} = k_t \varepsilon \;\Rightarrow\; \frac{1}{R}\frac{dt}{d\alpha} = k_t \frac{T}{EA} \tag{7}$$

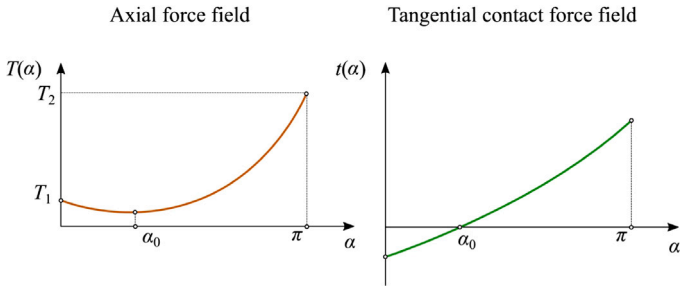

Fig. 5. Axial force and tangential contact force distributions.

where s is the arc-length coordinate along the rope centreline and EA is the axial stiffness of the rope. Substituting the lower equation of the right-hand side of Eq. (1) yields:

$$T'' - \frac{k_t R^2}{EA} T = 0 \tag{8}$$

This is a second order differential equation with constant coefficients in terms of the axial force distribution T. The solution is given by:

$$\begin{aligned} T(\alpha) &= T_a e^{r\alpha} + T_b e^{-r\alpha} \\ r &= \sqrt{\tfrac{k_t R^2}{EA}} \end{aligned} \tag{9}$$

where T_a and T_b are constants that can be calculated using the boundary conditions $T(0) = T_1$, $T(\pi) = T_2$, yielding:

$$T(\alpha) = T_a e^{r\alpha} + \left(T_1 - T_a\right) e^{-r\alpha}, \tag{10}$$

where

$$T_a = \frac{T_2 - T_1 e^{-r\pi}}{e^{r\pi} - e^{-r\pi}} \tag{11}$$

The tangential contact force field is proportional to the space derivative of $T(\alpha)$, yielding:

$$t(\alpha) = \frac{1}{R}\left(r T_a e^{r\alpha} - r\left(T_1 - T_a\right) e^{-r\alpha}\right) \tag{12}$$

At the cross-section where the tangential contact force is zero the axial force shows a minimum, as shown in Fig. 5. The angle where this cross-section is located is obtained as:

$$t(\alpha) = 0 \;\Rightarrow\; T_a e^{r\alpha_0} = \left(T_1 - T_a\right) e^{-r\alpha_0} \;\Rightarrow\; \alpha_0 = \frac{1}{2r} \log \frac{T_1 - T_a}{T_a} \tag{13}$$

Note that this angle α_0 can be out of the contact area. In that case the axial force does not show a minimum along the contact area.

3.2. Analytical solution with laterally elastic and axially elastic bristles

In computational mechanics, it may be convenient to consider that the bristles are also elastic in the axial direction. This method allows the calculation of the normal contact force distribution using an elastic approach as well. Just as normal contact force and axial force are coupled through the upper equation in the right-hand side of Eq. (1), the normal penetration d_n and the axial deformation ϵ are coupled similarly. Consider an infinitesimal slice of the rope that sinks a distance d_n in the surface of the sheave, as shown in Fig. 4. The undeformed length of the centreline of the slice is $(R + 0.5 l_s) d\alpha$, where l_s is the width of the rope. As shown in the figure, if the slice were free to slip along the sheave surface, it would exceed the contour of the slice, but it cannot do it due to the presence of the neighbouring slices. Therefore, the axial deformation due to the sinking can be calculated as the original length of the centreline of the segment minus the "constrained" length of the sinked slice. Thus, the axial strain yields:

$$\epsilon_s = \frac{R d\alpha - \left(R - d_n\right) d\alpha}{R d\alpha} = \frac{d_n}{R} \tag{14}$$

where ϵ_s is the axial strain of the rope due to the sinking. The total strain of the rope, due to the axial force and due to the sinking yields:

$$\epsilon = \frac{T}{EA} + \frac{d_n}{R} = \left(\frac{1}{EA} + \frac{1}{k_n R^2}\right) T \tag{15}$$

where the equations $d_n = p/k_n = T/(Rk_n)$ have been used. A fictitious axial stiffness of the rope that accounts for the rope-sheave normal indentation can be defined as follows:

$$\frac{1}{EA^*} = \frac{1}{EA} + \frac{1}{k_n R^2} \quad \Rightarrow \quad EA^* = \frac{EA + k_n R^2}{EAk_n R^2} \tag{16}$$

It is apparent that in this problem the axial stiffness of the centreline and the normal stiffness of the rope surface act as spring in series. The solution of the rope-sheave contact in the case of laterally elastic bristles, given in Eqs. (10) and (12), remains valid just substituting the exponent r given in Eq. (9) with this one:

$$r = \sqrt{\frac{k_t R^2}{EA^*}} \tag{17}$$

3.3. Energy balance

To check the validity of the solution, the *Principle of Work and Energy* is evaluated symbolically. The work of the applied forces equals the deformation energy of the rope:

$$W_{app} = U_{def} \tag{18}$$

The work of the apply forces is simply given by:

$$W_{app} = -\frac{1}{2}T_1 u(0) + \frac{1}{2}T_2 u(\pi) = \frac{1}{2k_t}\left(-T_1 t(0) + T_2 t(\pi)\right), \tag{19}$$

where the first equation of Eq. (7) has been used. This work is given by the following closed form:

$$W_{app} = \frac{r\left[\left(1 + e^{2r\pi}\right)\left(T_1^2 + T_2^2\right) - 4T_1 T_2 e^{r\pi}\right]}{2Rk_t\left(e^{2r\pi} - 1\right)} \tag{20}$$

The deformation energy of an infinitesimal slice of the rope includes the axial deformation energy of the rope, the axial deformation energy of the bristles and the transverse deformation energy of the bristles, as follows:

$$dU_{def} = dU_{ax} + dU_{nor} + dU_{tan} = \left(\frac{1}{2}EA\varepsilon^2 + \frac{1}{2}k_n\delta_n^2 + \frac{1}{2}k_t\delta_t^2\right)Rd\alpha \tag{21}$$

This expression can be easily written in terms of the axial force field $T(\alpha)$ and the tangential contact force field $t(\alpha)$, yielding:

$$dU_{def} = \left[\frac{1}{2}\left(\frac{1}{EA} + \frac{1}{R^2k_n}\right)T^2(\alpha) + \frac{1}{2}\frac{1}{k_t}t^2(\alpha)\right]Rd\alpha \tag{22}$$

The total deformation energy of the rope is obtained as the integral of the differential deformation energy, as follows:

$$U_{def} = \frac{1}{2}\left(\frac{1}{EA} + \frac{1}{R^2k_n}\right)\int_0^\pi T^2(\alpha)\,d\alpha + \frac{1}{2}\frac{R}{k_t}\int_0^\pi t^2(\alpha)\,d\alpha \tag{23}$$

The close form solution of this equations can be easily obtained using symbolic computation. The result is identical to the expression of the work of the applied forces given in Eq. (20). Thus, the fulfilment of the Principle of Work and Energy of the presented solution is proven.

4. Onset of the rope-sheave slipping and contact with partial slip

The analytical solution has physical meaning if the tangential contact force is at all sections smaller than the coefficient of friction μ times the normal contact force $p(\alpha)$. The numerical evaluation of the presented result shows that as T_2 increases, keeping all other terms constant, the tangential contact force field increases and the angle α_0 moves to the left and becomes negative. This tendency will be shown in the next section. That means that $t(\alpha)$ becomes positive all along the rope and the axial force $T(\alpha)$ does not show any minimum in the contact area (see Fig. 5). That means that both functions $t(\alpha)$ and $\mu p(\alpha)$ grow monotonically with increasing slope when α increases. Necessarily, the point where the slip begins is located at the end $\alpha = \pi$. The contact conditions when slip starts at that end are called here *onset of slipping*. The value of T_2 when these conditions are met can be calculated solving the equation:

$$t(\pi) = \mu p(\pi) \tag{24}$$

Using the expressions given in Eqs. (10) and (12), and considering the definition of T_a given in Eq. (11), the following result is easily obtained:

$$T_2^{onset} = \frac{2r}{r\left(e^{-r\pi} + e^{r\pi}\right) + \mu\left(e^{-r\pi} - e^{r\pi}\right)}T_1 \tag{25}$$

The contact conditions in the onset of slipping is represented in the central plot of Fig. 6. Only the section at $\alpha = \pi$ has reached the saturated tangential friction force.

The axial force at this end can still be increased before gross slipping of the rope starts. For values of the load such that $T_2^{onset} < T_2 < T_2^{gross}$ part of the rope at the high-load side achieves the saturated tangential force while the other part of the

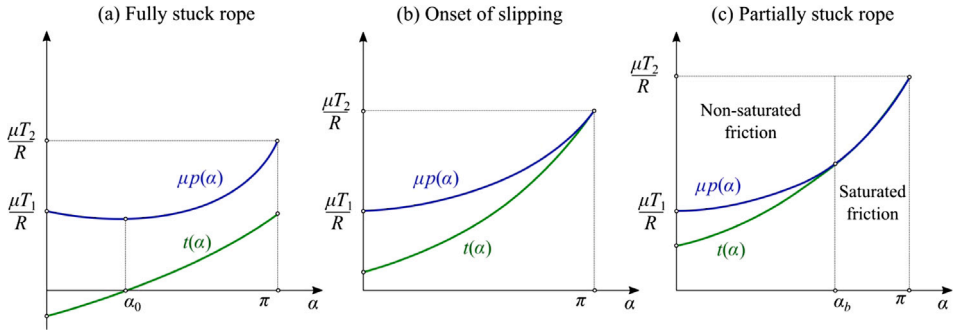

Fig. 6. Phases of rope-sheave contact in static conditions.

rope at the low-load side remains stuck to the sheave. Contact conditions are represented in the right plot of Fig. 6. The normal and tangential contact force distributions are calculated next.

To calculate the contact force fields, an angle α_b is assumed to limit the regions of saturated and non-saturated tangential contact forces. The axial force and tangential contact force distributions are assumed in the form:

$$\begin{aligned} T(\alpha) &= \begin{cases} T_I e^{r\alpha} + T_{II} e^{-r\alpha} & \text{if} \quad 0 \le \alpha < \alpha_b \\ T_b e^{\mu(\alpha-\alpha_b)} & \text{if} \quad \alpha_b \le \alpha \le \pi \end{cases} \\ t(\alpha) &= \begin{cases} \frac{r}{R}\left(T_I e^{r\alpha} - T_{II} e^{-r\alpha}\right) & \text{if} \quad 0 \le \alpha < \alpha_b \\ \frac{\mu}{R} T_b e^{\mu(\alpha-\alpha_b)} & \text{if} \quad \alpha_b \le \alpha \le \pi \end{cases} \end{aligned} \tag{26}$$

where T_I, T_{II}, T_b, and α_b are constants to be determined. Clearly, the expressions used in this equations are of the same form than the distributions obtained for the gross slipping and fully stuck distributions calculated in Sections 2 and 3, respectively.

Imposing boundary conditions on $T(\alpha)$ and continuity of the axial force and tangential contact force distributions, the following set of equations are obtained:

$$\begin{aligned} &T_I + T_{II} = T_1 \\ &T_I e^{r\alpha_b} + T_{II} e^{-r\alpha_b} = T_b \\ &r T_I e^{r\alpha_b} - r T_{II} e^{-r\alpha_b} = \mu T_b \\ &T_b e^{\mu(\pi-\alpha_b)} = T_2 \end{aligned} \tag{27}$$

The first three equations are linear in terms of T_I, T_{II}, T_b, and they can be used to obtain these constants as a function of the fourth one, α_b, as follows:

$$\begin{bmatrix} 1 & 1 & 0 \\ e^{r\alpha_b} & e^{-r\alpha_b} & -1 \\ r e^{r\alpha_b} & -r e^{-r\alpha_b} & -\mu \end{bmatrix} \begin{bmatrix} T_I \\ T_{II} \\ T_b \end{bmatrix} = \begin{bmatrix} T_1 \\ 0 \\ 0 \end{bmatrix} \Rightarrow \begin{cases} T_I = T_I(\alpha_b) \\ T_{II} = T_{II}(\alpha_b) \\ T_b = T_b(\alpha_b) \end{cases} \tag{28}$$

Substituting $T_b(\alpha_b)$ in the fourth equation of Eq. (27) yields:

$$T_b(\alpha_b)\, e^{\mu(\pi-\alpha_b)} = T_2 \quad \Rightarrow \quad \alpha_b = \pi - \frac{1}{\mu} \log \frac{T_2}{T_b(\alpha_b)} \tag{29}$$

The equation in the right-hand side is a non-linear equation that is very simple to solve numerically to find α_b. Once α_b is obtained, its value is substituted in Eq. (28) to find T_I, T_{II} and T_b. Thus, the axial force and tangential contact force distributions given in Eq. (26) become fully defined. Note that the all the results presented in this paper are purely analytical, closed-form solutions, with the only exception of this step, that requires a numerical iterative procedure, but it is elementary.

The numerical solution of Eq. (29) when T_2 varies continuously from T_2^{onset} to T_2^{gross} provides an angle α_b that varies continuously and smoothly from π to 0, as expected.

5. Example

In this section, the results presented in this paper are applied to a particular example whose parameters are defined in Table 1. To get the plots shown in this section, the high load T_2 is varied from T_1 up to T_2^{gross} using a small set of discrete values. Then, the normal and tangential contact force distributions are evaluated using the corresponding formulas developed in this paper as a function of α and then plotted. In this problem $T_2^{onset} = 2.77$ KN and $T_2^{gross} = 3.51$ KN. The selected discrete values for T_2 are:

$$T_2 \in \left[\ 1 \quad 1.5 \quad 2 \quad T_2^{onset} \quad 3 \quad 3.3 \quad T_2^{gross}\ \right] \quad \text{KN} \tag{30}$$

Fig. 7 shows the tangential contact forces and the normal contact forces multiplied by the coefficient of friction for values of T_2 smaller or equal T_2^{onset}. Some comments:

Table 1
Parameters of rope-sheave contact problem.

Parameter	Value
Low axial load, T_1	1 KN
Radius of sheave, R	0.3 m
Axial stiffness of rope, EA	40 MN/m
Transverse stiffness of bristles, k_t	20 MN/m^2
Axial stiffness of bristles, k_n	150 MN/m^2
Friction coefficient, μ	0.4

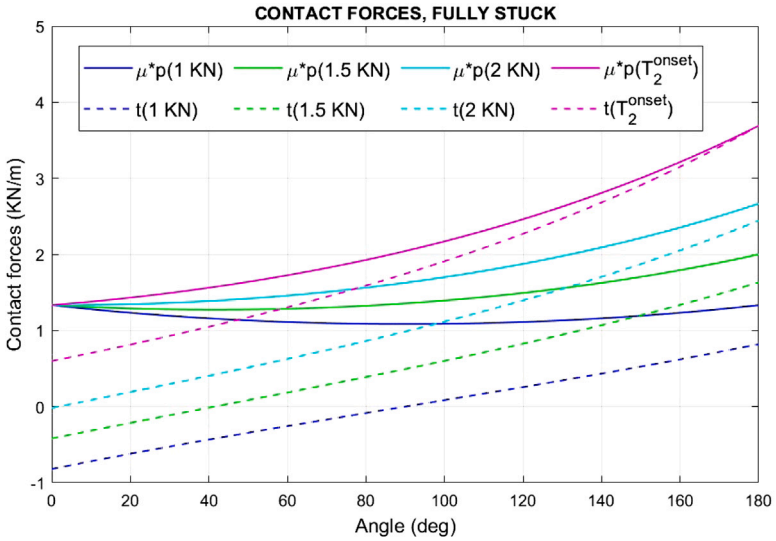

Fig. 7. Contact force distributions with rope fully stuck at the sheave.

- For $T_2 = T_1$ the normal contact force is symmetric and the tangential contact force anti-symmetric.
- For low values of T_2 the tangential contact force seems to be linear, but it is not.
- For relatively high values of T_2, in this case $T_2 > 2$ KN approximately, the tangential contact force does not change sign and the normal contact force does not show a relative minimum in the contact area
- It can be observed that for $T_2 = T_2^{onset}$ then $t(\pi) = \mu p(\pi)$.

Fig. 8 shows the tangential contact forces and the normal contact forces multiplied by the coefficient of friction for values of T_2 such that $T_2^{onset} \leq T_2 \leq T_2^{gross}$. Some comments:

- Normal and tangential contact force functions for $T_2 \geq T_2^{onset}$ do not have high order continuity at $\alpha = \alpha_b$, since they are piecewise functions, as shown in Eq. (26).
- For $T_2 = T_2^{gross}$ both curves fully overlap. This is why the tangential contact force curve cannot be observed in the plot.

6. Summary and conclusions

This paper presents an analytical solution to the rope-sheave contact problem in static conditions. The sheave is assumed to be locked and the rope is subjected to unequal axial loads at its two ends, $T_1 \leq T_2$. To find the analytical solution, the rope is assumed as linearly elastic in the axial direction without bending stiffness. Contact is analysed using a bristle model and Coulomb friction. The analytical solutions are valid in two different ranges of axial loads. For values of the high load T_2 smaller than the onset of slipping, $T_2 \leq T_2^{onset}$, the rope is fully stuck at the sheave. The axial force field and the normal and tangential contact force fields are exponential functions that depend on a characteristic exponent r that is a simple function of the axial stiffness of the rope and the normal and tangential stiffness of the bristles. For values of the high load T_2 larger than the onset of slipping but smaller than the load for gross slipping, $T_2^{onset} < T_2 < T_2^{gross}$, the analytic solutions for the axial force field and the normal and tangential contact force fields are piecewise exponential functions. Next to the low-load end, the solutions found for fully stuck rope remain valid, but next to the high-load end, the well known Euler-Eytelwin solution applies.

The mathematics used in the developments of this paper are elementary. Solutions are very simple, depend on very few parameters and can be reproduced by anyone. All solutions are fully analytical with the exception of the calculation of the angle

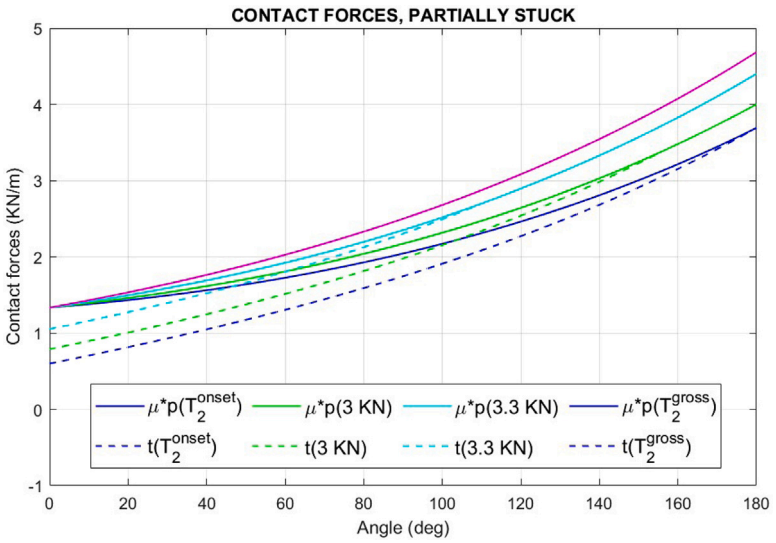

Fig. 8. Contact force distributions with rope partially stuck at the sheave.

that separates the stuck area of the slip area when $T_2^{onset} < T_2 < T_2^{gross}$. This angle has to be obtained numerically, but the equation is very simple.

The results presented in this paper can be applied in industrial applications if the normal and tangential contact stiffness of the assumed bristles, k_n and k_t, are identified. These values can be obtained with experimental tests. The analytical results presented in this paper have not been validated experimentally. The experiments that are needed to measure rope-sheave contact forces are technically difficult. The experimental results that are published in the scientific literature do not include the static rope-sheave contact forces. However, the experimental setup used by Usabiaga et al. [16] would be perfect for this application. Unfortunately, there is no access to that equipment.

The results presented in this paper have at least two applications. On the one hand, in the elevator industry, the implementation of new technologies that modify the ride of the system require the design engineers to demonstrate safety according to the standards [3]. These modifications usually involve the start and the stop of the cabin/counterweight. Understanding the rope-sheave static contact conditions is the first step to analyse the transition to dynamic contact conditions during the ride. In fact, this paper has been developed because of the calculations made by the author when working in safety analysis with the elevator industry. On the other hand, the bristle model, or its variants, is very commonly used nowadays in computational mechanics to simulate contact problems. The results presented in this paper can be used as a reference solution for the static simulation of the rope-sheave contact problem in computational mechanics.

Declaration of competing interest

The authors declare that they have no known competing financial interests or personal relationships that could have appeared to influence the work reported in this paper.

Data availability

No data was used for the research described in the article

Acknowledgements

This project has received funding from the European Union's Horizon 2020 research and innovation programme under the Marie Skłodowska-Curie grant agreement No 860124, THREAD.

European Commission
Horizon 2020
European Union funding
for Research & Innovation

Disclaimer

The present paper only reflects the author's view. The European Commission and its Research Executive Agency (REA) are not responsible for any use that may be made of the information it contains.

References

[1] L. Euler, Remarque sur L'Effet Du Frottement Dans L'Equilibre, Memorie de l'academie des sciences de Berlin, 1762, pp. 265–278.
[2] K.L. Johnson, Contact Mechanics, Cambridge University Press, Cambridge, UK, 1987.
[3] European Committee for Standarization, European standard EN 81-1, in: Safety Rules for the Construction and Installation of Lifts - Part 1. Electric Lifts, 1998.
[4] O. Reinolds, The engineer, 38, 396, 1847.
[5] F. Grashof, Theoretische maschinenlehre- band, 2, 1883, pp. 304–324.
[6] T.C. Firbank, Mechanics of the belt drive, Int. J. Mech. Sci 12 (12) (1970) 1053–1063.
[7] F. Frendo, F. Bucchi, Brush model for the analysis of flat belt transmissions in steady-state conditions, Mech. Mach. Theory 143 (2020).
[8] F. Frendo, F. Bucchi, Enhanced brush model for the mechanics of power transmission in flat belt drives under steady-state conditions: Effect of belt elasticity, Mech. Mach. Theory 153 (2020).
[9] F. Frendo, F. Bucchi, Validation of the brush model for the analysis of flat belt transmissions in steady-state conditions by finite element simulation, Mech. Mach. Theory 167 (2022).
[10] S. Chowdhury, R.K. Yedavalli, Dynamics of belt pulley shaft systems, Mech. Mach. Theory 98 (2016).
[11] S.R. Heller, The contact pressure between rope and sheave, Nav. Eng. J. (1970) 49–57.
[12] K. Feyrer, Wire Ropes. Tension, Endurance Reliability, Springer, 2007.
[13] A. Konyukhov, Contact of ropes and orthotropic rough surfaces, J. Appl. Math. Mech. 95 (4) (2015) 406–423.
[14] B. Häberle, Pressung zwischen Seil und Seilrille (Ph.D. thesis), University of Stuttgart, 1995.
[15] S. Nabijou, R.E. Hobbs, Frictional performance of wire and fibre ropes bent over sheaves, J. Strain Anal. 30 (1) (1995) 45–57.
[16] H. Usabiaga, M. Ezkurra, M.A. Madoz, J.M. Pagalday, Experimental test for measuring the normal and tangential line contact pressure between wire rope and sheaves, Exp. Tech. (2008).
[17] L. Della Pietra, F. Timpone, Tension in a flat belt transmission: experimental investigation, Mech. Mach. Theory 70 (2013) 129–156.
[18] K.U. Lee, S. Ahn, D.G. Hyun, T.W. Seo, Postion prediction of viscoelastic rope on traction sheave with rope-slip model, Mech. Mach. Theory 180 (2023).
[19] M.J. Leamy, T.M. Wasfy, Analysis of belt-drive mechanics using a creep-rate-dependent friction law, J. Appl. Mech. 69 (2002) 763–771.
[20] K. Kerkkänen, D. García-Vallejo, A. Mikkola, Modeling of belt-drives using a large deformation finite element formulation, Nonlinear Dynam. 43 (3) (2006) 239–256.
[21] G. Cepon, M. Boltezar, Dynamics of a belt-drive system using a linear complementarity problem for the belt–pulley contact description, J. Sound Vib. 319 (2009) 1019–1035.
[22] V.A. Lubarda, Determination of the belt force before the gross slip, Mech. Mach. Theory 83 (2015) 31–37.
[23] E. Oborin, Y. Vetyukov, I. Steinbrecher, Eulerian description of non-stationary motion of an idealized belt-pulley system with dry friction, Int. J. Solids Struct. 147 (2018) 40–51.
[24] E. Oborin, Belt-pulley interaction: role of the action line of friction forces, Acta Mech. 231 (2020) 3979–3987.
[25] U. Lugrís, J.L. Escalona, D. Dopico, J. Cuadrado, Efficient and accurate simulation of the rope-sheave interaction in weight-lifting machines, IMechE J. Multi-Body Dyn. 225 (2011) 331–343, Special Issue Paper.
[26] R. Bulín, Hajžman, P. Polach, Nonlinear dynamics of a cable-pulley system using the absolute nodal coordinate formulation, Mech. Res. Commun. 82 (2017) 21–28.
[27] G. Fotland, C. Haskins, T. Røvåg, Trade study to select best alternative for cable and pulley simulation for cranes on offshore vessels, Sys. Eng. 23 (2020) 177–188.
[28] Y. Guo, D. Zhang, X. Zhang, D. Wang, S. Wang, A new transmission theory of global dynamic wrap angle for friction hoist combining suspended and wrapped wire rope, Appl. Sci. 10 (2020) 1305.
[29] J.L. Escalona, H.A. Hussien, A.A. Shabana, Application of the absolute nodal coordinate formulation to multibody system dynamics, J. Sound Vib. 214 (5) (1998) 833–851.
[30] J.L. Escalona, An arbitrary Lagrangian-Eulerian discretization method for modelling and simulation of reeving systems in multibody dynamics, Mech. Mach. Theory 112 (2017) 1–21.
[31] J.L. Escalona, G. Orzechowski, A. Mikkola, Flexible multibody modelling of reeving systems including transverse vibrations, Multibody Syst. Dyn. 44 (2018) 107–133.
[32] J.L. Escalona, N. Mohammadi, Advances in the modeling and dynamic simulation of reeving systems using the arbitrary Lagrangian–Eulerian modal method, Nonlinear Dynam. 108 (2022) 3985–4003.
[33] D.A. Haessig, B. Friedland, On the modelling and simulation of friction, J. Dyn. Syst. Meas. Control. Trans. 113 (3) (1991) 354–362.
[34] C. Canudas de Wit, H. Olsson, K.J. Åström, P. Lischinsky, A new model for control of systems with friction, IEEE Trans. Automat. Control 40 (3) (1995) 419–425.